

Comparison of Luminous Intensity Distributions

Lerch, David; Trampert, Klaus; Neumann, Cornelius

Karlsruher Institute for Technology (KIT), Light Technology Institute (LTI)

Engesserstraße 13, Geb. 30.34, 76131 Karlsruhe

Tel. 0721 608-47383, david.lerch@kit.edu, www.lti.kit.edu

Abstract

If headlights for automobiles are put on the market, legal requirements must be complied with. Whether the oncoming traffic is dazzled by the headlights can be determined from the luminous intensity distribution curve (LID). For this, the so-called cut-off line must be determined. A declaration of conformity is only possible if the uncertainties of all sizes are considered.

A measured value in the LID consists of a direction, the solid angle, and an amount, the luminous intensity. If you represent each value of the LID as a vector and interpolate the support points, you get the luminous intensity body. When comparing LIDs according to the prior art, the luminous intensities are compared in pairs for each solid angle.

During a measurement, the position of the object in the measurement coordinate system is unknown, for example due to misalignment. As a result, the object coordinate system is shifted to the measurement coordinate system and a pairwise comparison is not expedient for each spatial direction.

If LIDs are compared on the basis of the intrinsic properties of the LID body, the orientation of the LID can be found in the measurement coordinate system. The aim of this work is to compare two LIDs based on the intrinsic properties of the LID body.



1 Motivation

In this work an approach is developed with which light distribution curves (LID) of the same luminaire are compared with one another. If two identical luminaires from different laboratories are to be measured, it is difficult to compare the two measurements.

When measuring a LID in the far field, it is important to know the exact center of light of the luminaire to be measured. It could be shown that the position of the center of light during a measurement has a great influence on the photometric limit distance [5]. In addition, it was found that the greatest uncertainty contribution to the orientation between light source and receiver during a measurement is the uncertainty of the orientation of the light source [4].

For the development of a method with which LIDs can be compared whose luminaires are the same but are oriented differently during the measurement, measurements are required in which a luminaire is measured in different orientations.

Measuring different luminaires for different orientations is very time consuming. A LID generator is therefore to be developed with which luminaires can be measured virtually.

2 Related work

2.1 Synthetic LIDs

There have been publications on LID generators in the past. The LITG has published software, developed by Dipl.-Ing. Nils Haferkemper, with which the resulting light distribution can be obtained for a certain room geometry, position and geometry of the luminaire and illuminance [3]. This LID generator was developed for developers and users of light simulation programs. As part of this work, a generator is developed that has been optimized for metrological applications.

2.2 Comparison of LIDs

In recent years, the point-to-point comparison of measured values has become established for the comparison of LIDs. When comparing the LIDs of two identical luminaires, it is known that the LIDs to be compared are ideally identical.

This basic assumption enables an optimization approach in which the distance between the two LIDs is minimized. For this, one LID is chosen as a reference, while the second is the test LID.

Now the test LID is shifted so that the distance between the two LIDs is minimal. Due to the shift, the test LID requires values that lie between the measured values. These intermediate values are obtained by means of linear interpolation between the measured values [1, 2].

The optimization can be done by means of a systematic shift [1] with constant steps, or with the minimization of the quadratic error [2]. In Figure 1 a flow chart is presented that shows which preprocessing steps are necessary in order to compare the light distributions with one another.

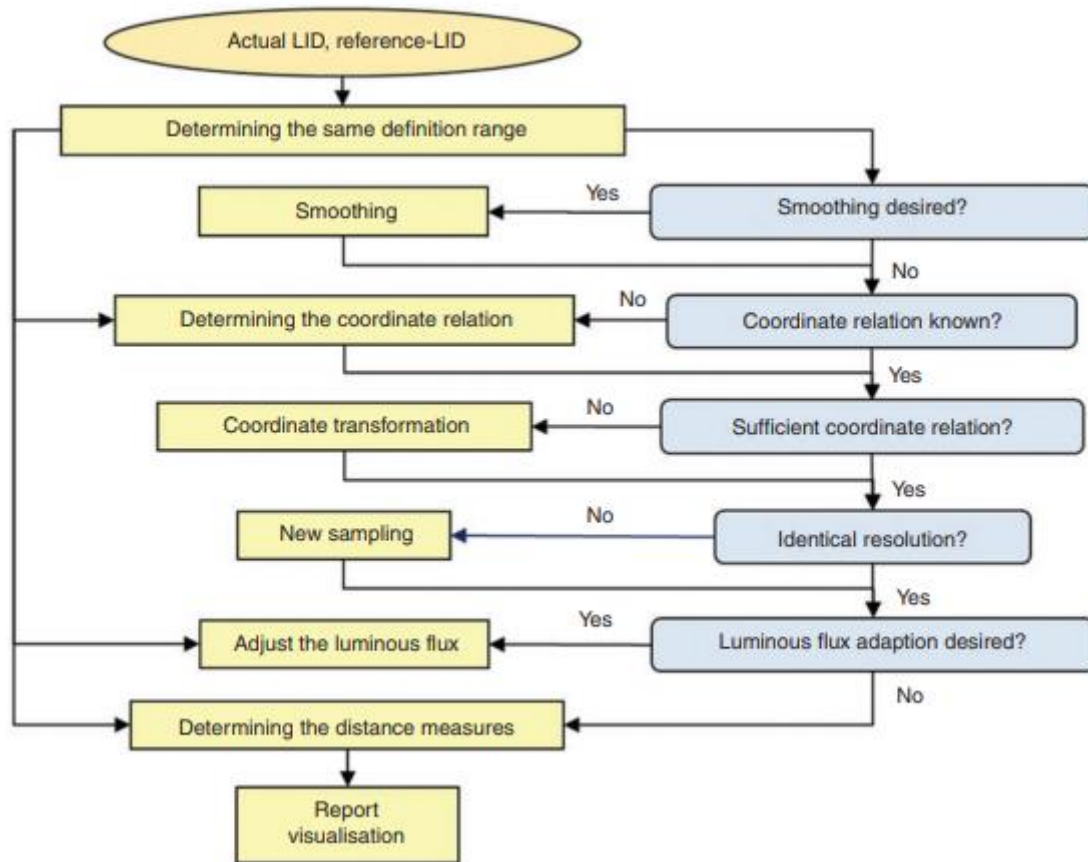


Figure 1: Flow chart for the comparison of LIDs [2]

3 Implementation

As part of this work, a framework was developed with which synthetic light distributions can be generated and measured virtually. For the artificial light distributions, analytical models were set up with which real light distributions can be approximated. Furthermore, features of LIDs are introduced.

3.1 Synthetic LIDs

In this work, a synthetic light distribution is composed of so-called cosine lobes. The shape of a cosine lobe is $\cos^n(\theta(\theta_k))$, with the form factor n of the radiation characteristic and the tilting angle θ_k of the lobe. For each lobe k a luminous flux Φ_k is determined. For each radiation direction i the luminous intensity is:

$$I_i = \sum_k \frac{\cos^{n_k}(\theta_i)}{\Phi'_k} * \Phi_k \quad (3.1)$$

With:

$$\begin{pmatrix} x'_i \\ y'_i \\ z'_i \end{pmatrix} = \begin{pmatrix} \sin \theta'_i \cos \varphi'_i \\ \sin \theta'_i \sin \varphi'_i \\ \cos \theta'_i \end{pmatrix} \quad (3.2)$$

$$\begin{pmatrix} x_i \\ y_i \\ z_i \end{pmatrix} = R \begin{pmatrix} x'_i \\ y'_i \\ z'_i \end{pmatrix} \quad (3.3)$$

$$R = R_z(\alpha)R_x(\beta)R_z(\gamma) = \begin{pmatrix} \cos \alpha \cos \gamma - \sin \alpha \cos \beta \sin \gamma & -\cos \alpha \sin \gamma - \sin \alpha \cos \beta \cos \gamma & \sin \alpha \sin \beta \\ \sin \alpha \cos \gamma + \cos \alpha \cos \beta \sin \gamma & -\sin \alpha \sin \gamma + \cos \alpha \cos \beta \cos \gamma & -\cos \alpha \sin \beta \\ \sin \alpha \sin \gamma & \sin \beta \cos \gamma & \cos \beta \end{pmatrix} \quad (3.4)$$

$$\alpha = \varphi_k, \beta = \theta_k, \gamma = \gamma_k$$

$$\theta_i = \frac{z_i}{\sqrt{x_i^2 + y_i^2 + z_i^2}} \quad (3.6)$$

$$\Phi'_k = \sum_i \cos^{n_k}(\theta_i) * \Omega_i \quad (3.7)$$

A synthetic light distribution can then be measured virtually. The C-plane system is used as the measuring coordinate system. To simplify the rotation, the coordinates of the C-plane system are converted into Cartesian coordinates and the rotations are carried out there.

This is followed by a reverse transformation into the C-level system. The optical axis points in the positive z-direction. The resolution of the measurement can be chosen arbitrarily.

In order to simulate squinting of the lamp, the measurement coordinate system is rotated on a spherical surface. For this, the formula (3.3) is extended by the rotation matrix R_m :

$$R_m \begin{pmatrix} x_i \\ y_i \\ z_i \end{pmatrix} = R \begin{pmatrix} x'_i \\ y'_i \\ z'_i \end{pmatrix} \quad (3.8)$$

The rotation matrix R_m has the same shape as the rotation matrix R in (3.4) with:

$$\alpha = \varphi_m, \beta = \vartheta_m, \gamma = \gamma_m$$

The angles φ_m , ϑ_m , γ_m define the position and orientation of the virtual measurement center ($C = 0$, $\gamma = 0$) on the surface of the measurement sphere. The default pose of the measurement center is on the z-axis with the angles:

$$\varphi_m = \vartheta_m = \gamma_m = 0$$

Instead of rotating the measurement center in world coordinates, the luminous intensity distribution is multiplied by the inverse rotation matrix of the measurement center:

$$\begin{pmatrix} x_i \\ y_i \\ z_i \end{pmatrix} = R_m^{-1} R \begin{pmatrix} x'_i \\ y'_i \\ z'_i \end{pmatrix} \quad (3.9)$$

3.2 Features of LIDs

In the following, four features of LIDs are introduced. These features are statistic features of the measured values, and therefore generically applicable.

The *form factor* is a degree of narrowness of a light source. It is calculated by the sum of partial luminous fluxes normed to the total luminous flux. The luminous intensity I_i is a vector. The form factor is calculated as follows:

$$f_{form} = 100\% * \frac{|\sum_i I(\theta_i, \varphi_i) * \Omega(\theta_i, \varphi_i)|}{\sum_k \Phi_k} \quad (3.10)$$

The form factor equals 100% for a laser and 0% for an isotropic radiator.

The *radiation direction* is the argument of the sum of partial luminous flux. The luminous intensity $I(\theta_i, \varphi_i)_i$ is a vector. The radiation direction is calculated with the the luminous intensity vector and the solid angle Ω_i as followed:

$$\Phi_{res,arg} = \arg \left(\sum_i I(\theta_i, \varphi_i) * \Omega(\theta_i, \varphi_i) \right) \quad (3.11)$$

The *relative difference* of luminous flux is a measure for uniformity of the radiation characteristic of a luminaire. Since the relative difference can be calculated for full space, half space or any other segment of space, it is strongly depending on the segment to which it refers.

It can be calculated as the difference between measured luminous intensities and mean luminous intensity. The largest relative absolute difference of an arbitrary sequence is 0.5. The relative difference is normed to the total luminous flux. The relative absolute difference in a LID is defined as followed:

$$f_{dif,rel} = 100\% * (2 * \frac{\sum_i ||I(\theta_i, \varphi_i)| - \bar{I}| * \Omega(\theta_i, \varphi_i)}{\sum_k \Phi_k}) \quad (3.12)$$

$$\bar{I} = \frac{\sum_i |I(\theta_i, \varphi_i)| * \Omega(\theta_i, \varphi_i)}{\sum_i \Omega_i} \quad (3.13)$$

The relative difference of a LID is 0% for an isotropic radiator. The measure is multiplied by 2 to arrange values between 0% and 100%.

The *maximum difference* of a LID is a measure for uniformity of the radiation characteristic of a luminaire. Complementary to the relative difference the maximum difference indicates anomalies.

However, the maximum difference is calculated as the maximum difference between measured luminous intensities and the mean luminous intensity. Therefore, it is strongly dependent of the spatial segment to which it refers. The calculation of the maximum difference of a LID is as followed:

$$f_{dif,max} = 100\% * \frac{\max(|I(\theta_i, \varphi_i)| - \bar{I})}{\max(I(\theta_i, \varphi_i))} \quad (3.14)$$

4 Comparison of different LIDs

In the following, the features developed within the scope of this work are evaluated. The light distributions generated by the LID generator are displayed as 2D projections. In addition, the properties of LIDs presented in section 3.2 for the generated light distributions are evaluated. All virtual measurements take place in full space, even if the radiation source radiates into a half space. The angular resolution of the virtual measurements is $\Delta\theta = \Delta\varphi = 2.5^\circ$.

4.1 Lambertian radiator

The ideal Lambertian radiator is modeled by the generator as a $\cos^1(\theta(0))$ lobe. The resulting LID is shown in figure 2. For this illustration the virtual measurement origin is set to:

$$\varphi_m = \theta_m = 0^\circ, \gamma_m = 90^\circ$$

The origin of the measurement is thus on the optical axis. The direction of radiation is in the direction of the optical axis ($\theta \approx 0$). For displacements of the measurement origin from the optical axis ($\theta_m \neq 0$), it is expected that the emitting direction $I_{res,arg}(\theta, \varphi)$ follows the measurement origin $(\varphi_m, \theta_m, \gamma_m)$ in angle θ .

The azimuth angle of the radiation direction behaves inverse (see formula (3.9)) to the measurement origin, with:

$$\gamma_m = -\varphi$$

By shifting the origin of the measurement, a squint of the luminaire from the optical axis is simulated.

Table 1 shows that the displacement of the measurement origin in the direction of emission is found. If the measurement origin is shifted by $\theta_m = 4^\circ$ or $\theta_m = 11^\circ$ respectively, the error in determining the inclination angle of the radiation direction is less than 1%. Both the form factor and the relative difference and the maximum difference are invariant to the displacement of the measurement origin.

The results shown for the ideal Lambertian radiator show that the selected properties are suitable for LIDs in order to compare tilted LIDs with one another. It should now be shown that the properties of the measured values are sensitive to white Gaussian noise.

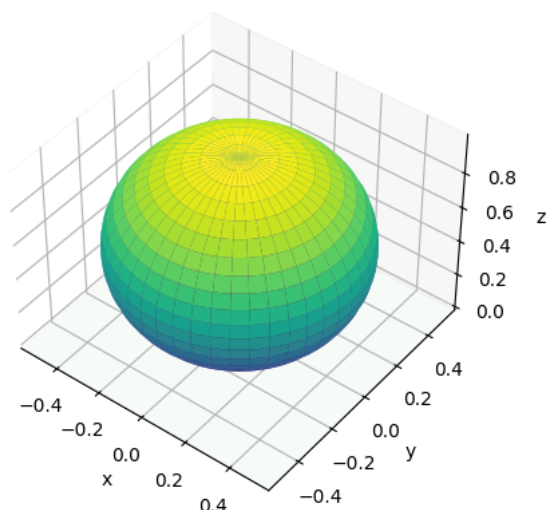


Figure 2: Illustration of the LID of and ideal measured Lambertian radiator

The determination of the inclination angle of the emission direction is made more difficult by white noise on the measured values. From table 2 it can be seen that the determination for a squint of 4° works significantly worse than for a squint of 11° .

Table 1: Features of the LID of an ideal measured Lambertian radiator

Measurement origin [°] ($\varphi_m, \theta_m, \gamma_m$)	$I_{res,arg}(\theta, \varphi)$ [°]	f_{form} [%]	$f_{dif,rel}$ [%]	$f_{dif,max}$ [%]
(0, 0, 90)	(0.00, 159.15)	66.23	17.79	75.00
(0, 4, 90)	(4.00, -90.00)	66.21	17.78	74.99
(0, 11, 90)	(11.00, -90.00)	66.22	17.78	74.99

This is contrary to the trend from table 1 and can be attributed to the noise of the measured values. Since there are no negative luminous intensity values, the value range of the luminous intensity values is limited to zero.

Since the noise is added in all spatial directions, so that luminous intensity values are greater than zero in the rear half-space as well, the form factor becomes smaller due to white noise. Furthermore, the relative difference is greater, since the positive

luminous intensity values in the rear half-space also influence the relative difference here.

Table 2: Features of Lambertian radiator with additive $N(0, 0.01)$ noise

Measurement origin [°] ($\varphi_m, \theta_m, \gamma_m$)	$I_{res,arg}(\theta, \varphi)$ [°]	f_{form} [%]	$f_{dif,rel}$ [%]	$f_{dif,max}$ [%]
(0, 0, 90)	(0.02, -116.78)	65.84	17.70	75.42
(0, 4, 90)	(4.00, -90.03)	65.81	17.69	75.43
(0, 11, 90)	(11.00, -90.08)	65.83	17.70	75.29

In contrast to the form factor and the RAD, the maximum difference decreases. Since the luminous intensity values must be greater than zero, the applied noise is no longer without mean values. The maximum luminous intensity increases, the average luminous intensity remains almost the same. This makes the maximum error smaller.

4.2 Narrow light sources

A bundled light source of the form $\cos^{10}(\theta(0))$ is now considered. The behavior of the properties of LIDs shown in chapter 4.1 for an ideal Lambertian radiator should now be evaluated for a simulated bundled light source.

Figure 3 shows the light distribution body of this light source. For the \cos^{10} -emitter, the tests are also carried out for the ideal luminous intensity values and noisy values. The results are summarized in tables 3 and 4.

The inclination angle θ of the radiation direction $I_{res,arg}$ is found just as well with the bundled light source as with the Lambertian emitter. The azimuth angle φ of the emission direction can be found more easily with the bundled light source. The clearly narrower radiation characteristic enables a better spatial allocation.

As expected, the form factor of the bundled source is significantly larger than that of the Lambertian radiator. In addition, the relative difference and maximum error are

significantly higher compared to Lambert's radiators. However, all of the properties listed are also independent of the squint of the virtual lamp in this case.

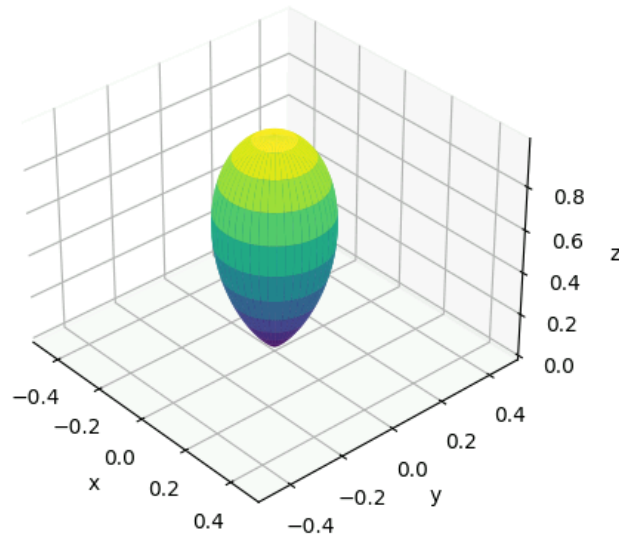


Figure 3: Illustration of the LID of an ideal measured \cos^{10} -radiator

If the \cos^{10} -emitter points out of the optical axis, the inclination angle of the emission direction is found to an accuracy of 0.05° . In addition, as with the Lambertian radiator, the form factor and the relative difference measure decrease with additive white noise. The maximum difference decreases as well. Thus, the maximum difference shows a different behavior for \cos^1 - and \cos^{10} -emitters.

Table 3: Features of the LID of an ideal measured \cos^{10} -radiator

Measurement origin [°] ($\varphi_m, \theta_m, \gamma_m$)	$I_{res,arg}(\theta, \varphi)$ [°]	f_{form} [%]	$f_{dif,rel}$ [%]	$f_{dif,max}$ [%]
(0, 0, 90)	(0.00, 160.73)	91.04	26.35	95.45
(0, 4, 90)	(4.00, -90.00)	91.06	26.36	95.44
(0, 11, 90)	(11.00, -90.00)	91.15	26.38	95.44

Table 4: Features of a \cos^{10} -radiator with additive $N(0, 0.01)$ -noise

Measurement origin [°] ($\varphi_m, \theta_m, \gamma_m$)	$I_{res,arg}(\theta, \varphi)$ [°]	f_{form} [%]	$f_{dif,rel}$ [%]	$f_{dif,max}$ [%]
(0, 0, 90)	(0.08, -123.27)	89.62	26.10	95.26
(0, 4, 90)	(4.08, -89.94)	89.63	26.11	95.24
(0, 11, 90)	(11.00, -89.62)	89.65	26.11	95.23

4.3 Multi lobe light sources

In further investigations it should be shown that the proposed properties also apply to light distributions consisting of two lobes. To do this, a luminaire is first simulated which emits into the rear half-space with a \cos^1 - and into the front half-space with a \cos^{10} -characteristic. The light distribution body of this luminaire is shown in figure 4.

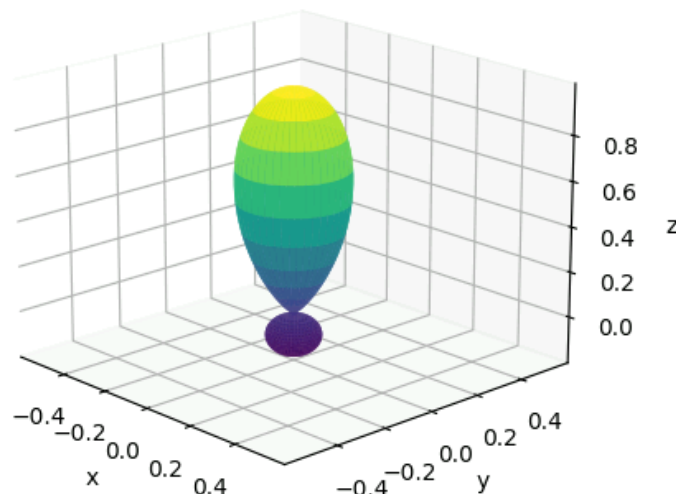


Figure 4: Illustration of an ideal measured full space radiator

Table 5 shows the properties of the LID. The direction of radiation is found significantly worse with this emitter than with the \cos^1 - or the \cos^{10} -emitter. The form factor, as well as the relative difference and maximum difference, also remain invariant to tilting in this case.

Now white Gaussian noise is also added to this radiator. As in the previous experiments, the direction of radiation is detected worse (see table 6). The form factor becomes larger due to the noise.

Table 5: Features of an ideal measured full space radiator

Measurement origin [°] ($\varphi_m, \theta_m, \gamma_m$)	$I_{res,arg}(\theta, \varphi)$ [°]	f_{form} [%]	$f_{dif,rel}$ [%]	$f_{dif,max}$ [%]
(0, 0, 90)	(0.00, -118.77)	12.40	15.26	90.90
(0, 4, 90)	(3.99, -90.00)	12.42	15.26	90.89
(0, 11, 90)	(10.98, -90.00)	12.46	15.27	90.89

Table 6: Features of a full space radiator with $N(0, 0.01)$ -noise

Measurement origin [°] ($\varphi_m, \theta_m, \gamma_m$)	$I_{res,arg}(\theta, \varphi)$ [°]	f_{form} [%]	$f_{dif,rel}$ [%]	$f_{dif,max}$ [%]
(0, 0, 90)	(0.69, 122.81)	12.81	15.15	91.00
(0, 4, 90)	(3.59, -92.92)	12.81	15.13	91.02
(0, 11, 90)	(10.76, -89.57)	12.88	15.15	90.96

This is due to the fact that more negative luminous intensity values are caused by the noise in the rear half-space. The negative values come from the fact that the variance of the noise is coupled to the maximum luminous intensity of the LID and is therefore given by the \cos^{10} -radiator.

However, negative luminous intensity values are set to 0, which means that the noise is no longer free of mean values. Therefore, the form factor increases with the noise.

With this light source, too, the relative difference and maximum difference behave analogously to the Lambertian radiator.

Next, consider a radiator that consists of two \cos^{10} -lobes, which are inclined at $\varphi = 0^\circ$ and $\varphi = 180^\circ$ by 20° from the optical axis. The associated luminous intensity distribution body is shown in Figure 5.

The properties for this light distribution are listed in table 7. The table shows that the inclination angle of the radiation direction is found very precisely. If the measuring surface is tilted by $\theta = 4^\circ$ or $\theta = 11^\circ$, the angle of inclination is found precisely.

The form factor, the relative difference and the maximum difference are also invariant to tilting for this LID. If the luminaire is additively superimposed with white noise, the direction of radiation is found with an accuracy of 0.02° (table 8).

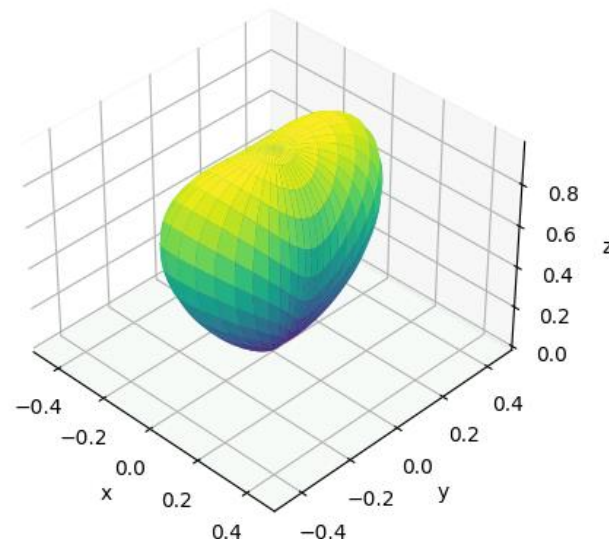


Figure 5: Illustration of a LID consisting of two narrow lobes each squinting 20° from the optical axis

For the last experiment, the \cos^{10} -lobes of the radiator are now tilted 50° from the optical axis. The associated luminous intensity distribution body is shown in figure 6.

With the simulation of this luminaire, the influence of a broad radiation and an ambiguous main radiation direction on the characteristics of a LID presented in this paper is to be examined.

The associated results can be found in table 9. With this LID, the direction of radiation can be determined very precisely.

As a result of the wide radiation, the azimuth angle of the radiation can now also be determined very precisely in addition to the angle of inclination. The angle of inclination can be determined with an accuracy of 0.02° , the azimuth angle with an accuracy of 0.05° . The form factor, the relative difference and the maximum difference are also invariant to tilting of this LID.

Table 7: Features of an ideal measured radiator consisting of two narrow lobes each squinting 20° from the optical axis

Measurement origin $[\circ]$ ($\varphi_m, \theta_m, \gamma_m$)	$I_{res,arg}(\theta, \varphi)$ $[\circ]$	f_{form} [%]	$f_{dif,rel}$ [%]	$f_{dif,max}$ [%]
(0, 0, 90)	(0.00, -37.34)	85.82	24.73	91.73
(0, 4, 90)	(4.02, -90.00)	85.82	24.73	91.74
(0, 11, 90)	(11.05, -90.00)	85.82	24.73	91.75

Table 8: Features of a LID consisting of two narrow lobes each squinting 20° from the optical axis with $N(0, 0.01)$ -noise

Measurement origin $[\circ]$ ($\varphi_m, \theta_m, \gamma_m$)	$I_{res,arg}(\theta, \varphi)$ $[\circ]$	f_{form} [%]	$f_{dif,rel}$ [%]	$f_{dif,max}$ [%]
(0, 0, 90)	(0.01, -26.70)	84.82	24.54	91.57
(0, 4, 90)	(4.03, -89.71)	84.79	24.54	91.62
(0, 11, 90)	(11.09, -90.11)	84.91	24.55	91.63

If this LID is superimposed with white Gaussian noise, the direction of radiation is significantly more robust compared to the previous light distributions. The form factor, the relative difference and the maximum difference measure show the same behavior in the case of noise as with the \cos^1 - and the \cos^{10} -emitter.

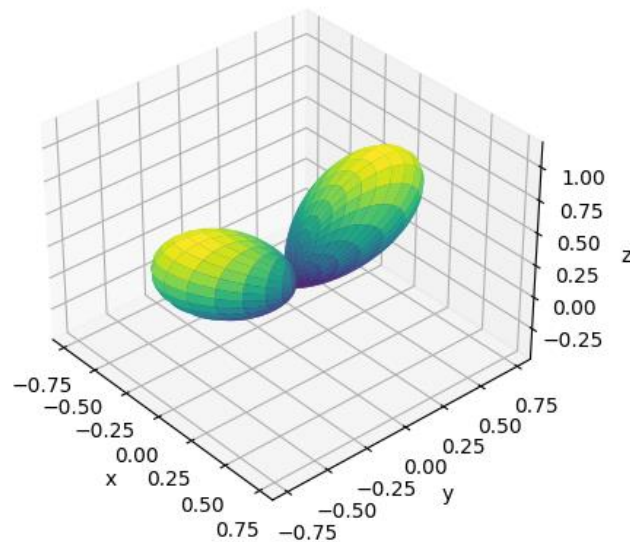


Figure 6: Illustration of a LID consisting of two narrow lobes each squinting 50° from the optical axis

Table 9: Features of an ideal measured radiator consisting of two narrow lobes each squinting 50° from the optical axis

Measurement origin [°] ($\varphi_m, \theta_m, \gamma_m$)	$I_{res,arg}(\theta, \varphi)$ [°]	f_{form} [%]	$f_{dif,rel}$ [%]	$f_{dif,max}$ [%]
(0, 0, 90)	(0.00, -54.88)	58.92	22.77	90.91
(0, 4, 90)	(4.01, -90.00)	58.92	22.77	90.90
(0, 11, 90)	(11.02, -90.00)	58.91	22.76	90.90

4.4 Discussion

In all cases, the calculated emitting direction follows the tilting of the initial LID. The error of the emitting direction is smaller than the angular resolution ($\Delta\theta = \Delta\varphi = 2.5^\circ$). However, the quality of the calculated emitting direction strongly depends on the magnitude of the form factor. If the form factor is close to zero, the radiation direction depends on noise.

The relative difference and the maximum difference of ideal measured LIDs are constant for tilting with less than 0.1% error. With noise, the values of the proposed features differ to the features of ideal measured LIDs.

This means that the properties can be used to compare two identical light distributions. On the basis of the properties presented, noise and squinting of the LID can be distinguished after the measurement.

Table 10: Features of a LID consisting of two narrow lobes each squinting 50° from the optical axis with $N(0, 0.01)$ -noise

Measurement origin [°] ($\varphi_m, \theta_m, \gamma_m$)	$I_{res,arg}(\theta, \varphi)$ [°]	f_{form} [%]	$f_{dif,rel}$ [%]	$f_{dif,max}$ [%]
(0, 0, 90)	(0.07, -87.99)	58.02	22.62	90.72
(0, 4, 90)	(4.10, -89.88)	58.06	22.60	90.80
(0, 11, 90)	(10.98, -90.06)	57.94	22.59	90.79

5 Summary and future work

For the comparison of LIDs, a feature-based approach was chosen in this paper in order to differ between systematic errors and stochastic uncertainties of the measured LIDs.

The presented method was evaluated on synthetic LIDs. The synthetic LIDs are manipulated to simulate systematic errors. In our approach synthetic LIDs are rotated. In order to find those rotations a mathematical formulation for the emitting direction is proposed. Moreover, rotation invariant features were presented.

The features presented are sensitive to noise and are therefore suitable for distinguishing between systematic errors, namely rotation errors, and stochastic uncertainties.

In a new version, the generator is supposed to simulate measurement errors due to incorrect positioning of the luminaire during the measurement. Incorrect calibration of the measurement distance and the resulting errors when calculating the luminous intensities should be considered.

Furthermore, there should be more investigation about the behavior of features regarding systematic errors and different distributions and magnitudes of noise.

In addition, it is possible to calculate the homogeneity and isotropy of LIDs based on histograms of luminous intensities. Histogram-based approaches are more robust and more general compared to single values.

Literatur

- [1] ASJ Bergen, „A practical method of comparing luminous intensity distributions,“ *Lighting, Research & Technology*, Vol. 44, Issue 1, pp. 27-36, 2012.
- [2] F Gassmann, U. Krueger, T. Bergen, F. Schmidt, „Comparison of luminous intensity distributions,“ *Lighting, Research & Technology*, Vol. 49, Issue 1, pp. 62-83, 2017.
- [3] N. Haferkemper, C. Vandahl, A. Stockmar, B. Hölzemann, „LVK-GENERATOR - Software zur Erzeugung virtueller Lichtstärkeverteilungen,“ *Deutsche Lichttechnische Gesellschaft e.V. (LiTG)*, ISBN 978-3-927787-55-1, 1. Auflage 2016.
- [4] M. Katona, K. Trampert, C. Neumann, „System analysis of ILMD-based LID measurements using Monte Carlo simulation,“ eingereicht bei *14th International Conference on New Developments and Applications in Optical Radiometry (NEWRAD 2021)*, 2021.
- [5] M. Katona, K. Trampert, C. Neumann, „Fehlerabschätzung der Fernfeldannahme bei LVK-Messungen mittels Nahfelddaten,“ *LICHT2021*, 2021.